



Calibration and Software Interface of an IQ-Mixer

by

Eugen Kammerloher

Bachelor's thesis in Physics

presented to

The Faculty of Mathematics, Computer Science and Natural Sciences at RWTH Aachen University

Department of Physics, Institute II C

July 2012

supervised by

Prof. Hendrik Bluhm, PhD

Contents

1	Introduction	5
2	Working model of an IQ mixer	6
2.1	Operating principles of a balanced mixer	6
2.2	Deviations from ideal mixer model	9
2.3	IQ mixer	10
3	Calibration	12
3.1	Calibration setup and calibration model	12
3.2	Calibration procedure	15
3.2.1	Calibration steps	15
3.2.2	Implementation	16
4	Measurements	18
4.1	Calibration results	18
4.2	Comparison of calibrated and uncalibrated mixer	23
4.2.1	Crosstalk	24
4.2.2	Amplitude	26
4.2.3	Frequency	30
4.2.4	Phase	33
5	Conclusion	36
6	Acknowledgments	37
7	Appendix	40
7.1	Calibration procedure	40
7.2	RF pulse creation	42

Conventions

The following conventions are used in this work:

V_{PP} is called a peak-to-peak voltage of a time variant signal.

V_P is half of V_{PP} and is equivalent to the amplitude of a sinusoidal signal.

V_{RMS} is the RMS voltage. For a sinusoidal signal it is equivalent to $\sqrt{2}V_{RMS} = V_P$.

dB is a logarithmic ratio of a physical quantity. The ratio L_{dB} in dB can be calculated for a ratio of powers:

$$L_{dB} = 10 \log_{10} \left(\frac{P_1}{P_0} \right).$$

dBm is the logarithmic ratio of power based on $P_0 = 1\text{mW}$.

1 Introduction

In the quest to harness quantum effects and revolutionize computing, there arise many new challenges. To build a device that works with wavefunctions, superpositions and the laws governing the quantum regime DiVincenzo formulated five important requirements [1], which have to be met in order to realize meaningful advantages of a so called quantum computer. This device would be assembled out of a number of qubits, the quantum analog of the digital bit and should meet the following criteria:

1. Qubits should be based on a scalable technology: it must be possible to fabricate large scale processors with many reliably functioning qubits.
2. It should be possible to initialize qubits into a known state.
3. The decoherence time, i.e. the time over which quantum information is retained, should be long compared to the time required for an operation.
4. It must be possible to execute a universal set of quantum gates. In other words, one must have full control over the qubits. Furthermore, these gates must fulfil certain accuracy requirements.
5. One must be able to read out the state of a qubit with high fidelity.

The current development of qubits is being investigated on a wide variety of physical devices [2], which each fulfil these requirements in some manner.

One approach is to use specially prepared semiconductor heterostructures [3] of Si, SiGe, GaAs/AlGaAs and other combinations, to benefit from the advanced state of the semiconductor processing industry. On such a semiconductor structure electrons may be trapped and controlled by lithographically defined metallic gates producing variable potential barriers and creating potential wells. The energy states of the trapped electrons are used to realise quantum two-level systems which form the basis of a qubit.

To achieve reasonable coherence times and good control on a qubit, the coupling of the trapped electron spin with the surrounding nuclear spin bath has to be taken into account. Spin-fluctuations of the large number of surrounding nuclei are a weak point of some semiconductor designs based on a host material with nonzero nuclear spin, particularly GaAs. But there exist a number of strategies to improve this problem [4], [5], [6].

A two level system driven by a matching EM-field will undergo Rabi flopping with oscillations between the two levels. In the case of an electron spin in a dot this flopping flips the spins of the surrounding nuclei and can be used to pump them [7], i.e. to change a large number of nuclear spins through repetitive Rabi flopping sequences in a controlled fashion. Such electron-nuclear flip-flop pumping cycles are controlled by voltages applied to the electrostatic gates.

ESR/EDSR in which a spin is driven in a fixed external/effective magnetic field allows coherent qubit manipulation with full control, achieved by using a sinusoidal signal when both frequency and phase can be adjusted.

Such a signal can be produced by a Vector Waveform Generator (VWG). However these instruments are expensive¹ and an alternative more economical approach to create a sinusoidal signal with controllable phase is desirable for operating with multiple qubits when a vector signal is required for each one.

The aim of this thesis is to assemble and calibrate a vector (sinusoidal) source using an IQ mixer. An IQ mixer is a widely used RF component, which is present in most modern wireless communication devices, that use frequency or phase modulation techniques for transmission and reception.

The basic operation of an IQ mixer is to manipulate the frequency and phase of an incoming RF signal dependent on two control inputs. Since the IQ mixer is subject to physical deviations the aim of this work is focused on creating a calibration procedure to predict the IQ mixers behaviour and to extend the existing software bundle Pulsecontrol² to create RF pulses of a desired amplitude, frequency and phase based on the measured calibration data. Additionally an frequency sweep can be generated. This can be used to robustly invert an electron spin [8].

2 Working model of an IQ mixer

This section explains how an ideal mixer would work and how component mismatches lead to deviations from ideal behaviour that affect its function for the specific example of a double balanced mixer. It is also explained how an IQ mixer can be composed of two double balanced mixers, as is the case with the Micro Circuits IQ-0307LXP used for the work in this thesis and what additional deviations can arise from the added complexity to this system.

2.1 Operating principles of a balanced mixer

The purpose of a mixer is to mix two time variant signals. This can be achieved by a multitude of different electronic circuits [9], [10]. Any non-linear component, for example, a diode, is able to do this. Figure 1 shows a simple mixer circuit that relies on the Shockley diode equation [11], which predicts an exponential relationship between current and voltage across the diode: $I \sim e^U$. A Taylor expansion for small voltages yields $I = U + \frac{U^2}{2} + \mathcal{O}(U^3)$.

A signal on the LO port $U_{\text{LO}}(t)$ is coupled to the IF port signal $U_{\text{IF}}(t)$. That means that the linear combination $\alpha U_{\text{LO}}(t) + \beta U_{\text{IF}}(t)$ now enters the diode, with α and β defining a fraction of the input signals (for simplicity assume $\alpha = \beta = 1$). The resulting current across

¹For example the E8267D PSG Vector Signal Generator from Agilent costs over EUR 80,000.

²Pulsecontrol can be measured from <http://code.google.com/p/special-measure/source/checkout?repo=pulsecontrol>. It is a part of Special Measure, a control software designed to provide a simple interface to control instruments and acquire data using MATLAB®. Pulsecontrol is used by the Bluhm and Stampfer groups of RWTH-Aachen to generate, maintain and upload pulse sequences for arbitrary waveform generators (AWGs).

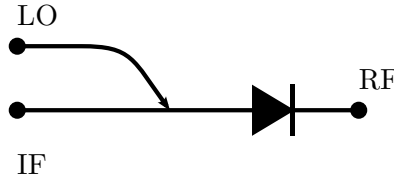


Figure 1: Simple single-ended mixer. LO: (local oscillator) a stable continuous wave input signal. IF: (intermediate frequency) input signal which typically has a small frequency. RF: (radio frequency) microwave signal containing the mixed signals.

the diode is: $I \sim U_{LO}(t) + U_{IF}(t) + \frac{U_{LO}^2(t)}{2} + \frac{U_{IF}^2(t)}{2} + U_{LO}(t)U_{IF}(t)$. It is dependent on the product of the two voltages. The fifth term is the desired mixed signal.

This simple setup has a few drawbacks. The output at the RF port needs to be filtered to obtain the mixed term while suppressing the other components of the output. There is no isolation between the LO-IF and LO-RF ports.

A more advanced setup is the double balanced mixer. Figure 2 shows an implementation using two pairs of diodes.

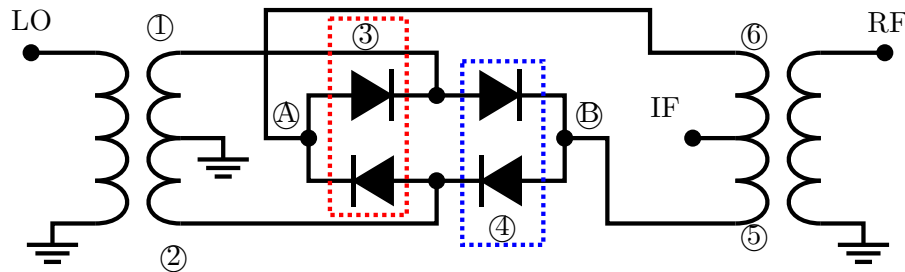


Figure 2: Double balanced mixer [12] consisting of two pairs of matched diodes (dotted boxes) and balanced inductive coupling of both the LO and RF port. The IF port is DC coupled.

At the heart of the mixer are two diode pairs ③ and ④. The LO input is inductively coupled into the setup. Since the inductance at the left is grounded in the middle the signal from LO ($U_{LO}(t)$) is split to two parts with $\frac{U_{LO}(t)}{2}$ at ① and a 180° phase shifted signal $-\frac{U_{LO}(t)}{2}$ at ②. Depending on the sign of the LO input either diode pair ③ or diode pair ④ conduct while the other pair is reverse biased and so isolates. Due to the two parts of the LO signal being 180° out of phase they cancel each other out at their crossing point ⑤ or ⑥, creating ground level.

Thus for positive $U_{LO}(t)$ ⑤ is held at zero volts, since diode pair ④ conducts. Diode pair ③ isolates, no current flows through ⑤. ⑥ is virtually disconnected from ground. For negative $U_{LO}(t)$ the reverse is true with ⑥ connected to ground at ⑤.

This type of mixer is called a switching mixer. It has good LO to RF isolation, since the

LO signal is nominally cancelled after the diode pairs at Ⓐ or Ⓑ. Furthermore, due to the inductive coupling, all ports are DC isolated from each other. While this is desirable for high LO and RF frequencies, it is a drawback when working with low frequencies, where the inductive coupling acts as a high pass filter.

It is important to note that while the IF port is an input and the RF port an output the two signal direction could be reversed. However the port are not interchangeable due to their coupling.

The IF port is DC coupled to the switching diodes and so the IF input can be either a constant DC voltage or a an AC signal. Coupling of the IF input to RF port switches between +1 and -1 according to the function: $\text{sgn}(x) = \frac{x}{|x|}$. This induces a signal in the RF coil and thus at the RF port: $U_{\text{RF}}(t) = U_{\text{IF}}(t) \text{sgn}(U_{\text{LO}}(t))$.

When the RF port is used as an input port the input frequency has to be comparatively large to pass the inductive coupling. The process is then analogue in the other direction: Either ⑤ or ⑥ is connected to ground depending on the function $\text{sgn} U_{\text{LO}}(t)$. Thus the signal from the RF coil induces an IF signal which switches in polarity and can be described as: $U_{\text{IF}}(t) = U_{\text{RF}}(t) \text{sgn}(U_{\text{LO}}(t))$.

For the purpose of frequency shifting a high frequency signal the first method is discussed in more detail and is used in the subsequent work. The sgn-function as defined above can be expanded in a Taylor series as a sum of cos-terms: $U_{\text{RF}}(t) = U_{\text{IF}}(t)(U_{\text{LO}} \cos(\omega_{\text{LO}}t) + \mathcal{O}(\cos^2(\omega_{\text{LO}}t)))$. For $U_{\text{IF}}(t) = U_{\text{IF}} \cos(\omega_{\text{IF}}t)$ this gives:

$$U_{\text{RF}}(t) = U_{\text{IF}} U_{\text{LO}} \cos(\omega_{\text{IF}}t) \cos(\omega_{\text{LO}}t) + \text{other terms}$$

which can be rewritten using trigonometric identities as:

$$U_{\text{RF}}(t) = \frac{U_{\text{IF}} U_{\text{LO}}}{2} [\cos((\omega_{\text{LO}} + \omega_{\text{IF}})t) + \cos((\omega_{\text{LO}} - \omega_{\text{IF}})t)] + \dots \quad (1)$$

The LO frequency is split off into two components at $(\omega_{\text{LO}} + \omega_{\text{IF}})$ and $(\omega_{\text{LO}} - \omega_{\text{IF}})$ plus higher harmonics. The signals at $\omega_{\text{LO}} \pm \omega_{\text{IF}}$ are called sidebands. Figure 3 illustrates the unfiltered output of a mixer. Often only one sideband is required and the other image sideband, is suppressed with a filter. The suppression is called image rejection.

An IQ mixer, which will be discussed in the section 2.3, has the image sideband filtered out, in a way that still enables rapid changes in frequency of the RF output.

But before that deviations of the previously introduced more simple case of a double balanced mixer from the pure $\cos((\omega_{\text{LO}} + \omega_{\text{IF}})t) + \cos((\omega_{\text{LO}} - \omega_{\text{IF}})t)$ form are discussed in the next subsection.

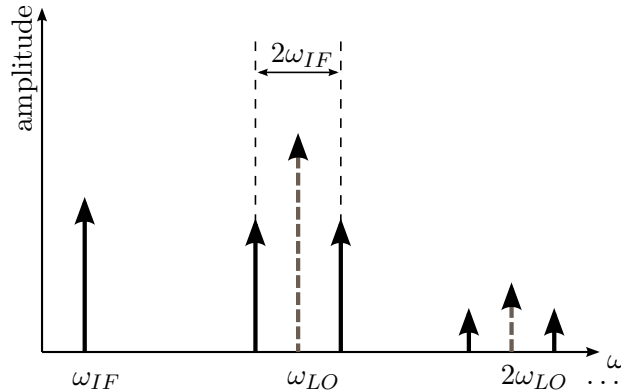


Figure 3: Schematic representation of a mixing process

2.2 Deviations from ideal mixer model

As may be expected with variation in real component the measured signal at the output port is not simply the sum of the two pure sidebands. Looking back at figure 2 there are several things to consider.

It was assumed, that the respective diode pairs completely cancel out the LO and the 180° shifted LO signals. If the impedance through the two diodes is not equal, a small portion of the LO signal is fed through to the RF port. The amount of LO signal feed-through also depends on the sign of the LO signal, since the diode pairs ③ and ④ will each have a different feed-through. Additional to this LO feed-through is crosstalk directly from the LO port to the RF port of high frequency LO signals, due to the small size of the circuit.

Another possible cause of non-ideal mixing is the division of the signal at the LO coil into the two branches ① and ②. If the middle ground-connection of the coil is not balanced the positive and negative component of the LO signal will be unequal and produce frequency dependent crosstalk proportional to $\text{sgn}(\sin(\omega_{\text{LO}} t))$. The same applies to the an imbalance in the position of the IF port on the IF coil. If the middle ground connection is not balanced the amplitude of the IF signal coupled into the RF coil will be similarly affected.

The sidebands are not precise single frequencies, but are smeared out due to noise in the system. Additional to the, presumably noisy, incoming LO and IF signals the diodes introduce noise depending on their temperature.

As seen in (1) the RF signal also contains higher harmonics of the sidebands. These harmonics distort the output signal which in an ideal mixer, with only the first order of the Taylor expansion., would not be present.

The inductive coupling of inputs introduces losses and since the diode tunnel barrier must be overcome to initiate current flow, the LO signal is needs to be of a sufficient amplitude. The IF signal is also inductively coupled and attenuated, but can be much lower, since it is stronger coupled to the RF signal.

As seen in the first simple mixer model (figure 1), diodes are non-linear components, introducing non-linear behaviour in this setup. This creates deviations from a linear RF amplitude response to the IF amplitude of the mixer for sufficiently strong IF signals.

The specific details of many sources of deviations of a double balanced mixer as discussed above can be summarized in four conventional values, which describe the main properties of a mixer and allow one to compare different mixers. These parameters are defined as follows:

conversion loss (dB)

This describes the ratio of the IF input power to the RF output power. It is strongly dependent on the LO signal power. A smaller conversion loss is better.

isolation (dB)

A global measure of the balance between the components of the mixer. It depends on the frequency range. The isolation is measured from LO to RF, RF to IF and LO to IF. A larger isolation is better.

1dB compression point (dBm)

The RF power at which the deviation from the low power, initially linear, relation of IF to RF power reaches -1dB. A high compression point means less deviation from linear behaviour.

third order intercept point (dBm)

This is a measure of non-linearity of the mixer. Using a signal consisting of two frequencies f_1 and f_2 it describes when the intermodulation product $m \cdot f_1 + n \cdot f_2$ of the order $|n| + |m| = 3$ would have the same amplitude as the original signal.

2.3 IQ mixer

An IQ mixer is a specific way to suppress the image sideband, called an image reject mixer. Figure 4 shows a schematic diagram. Two double-balanced mixers are shown by crossed circles. The LO signal enters the setup from the left and is split between the two mixers. The lower path is phase-shifted by 90° . LO_1 and LO_2 now enter the mixers on their LO ports. The functionality of the IQ mixing is achieved via the two IF ports I and Q, from which the mixer gets its name. The signal from the two RF ports is then combined and the resulting signal output at the RF port.

This functionality can be achieved by many electronic implementations. Only the effects and additional deviations introduced by the principal design are considered.

The names I and Q of the two IF ports stand for in-phase and quadrature-phase, a 90° shifted component. With an input $I(t) = U_{IF} \cos(\phi(t))$ on the I port and $Q(t) = U_{IF} \cos(\phi(t) + \frac{\pi}{2})$ on the Q port, the output at the RF port of an ideal IQ mixer is as follows:

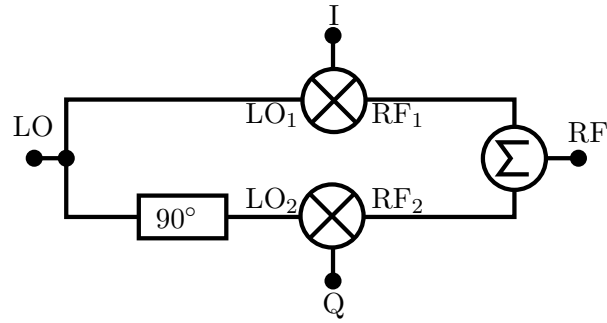


Figure 4: IQ mixer

$$\begin{aligned}
 U_{RF}(t) &= U_{LO} \left(I(t) \cos(\omega_{LOT}) + Q(t) \cos(\omega_{LOT} + \frac{\pi}{2}) \right) \\
 &= U_{LO} U_{IF} \left(\cos(\phi(t)) \cos(\omega_{LOT}) + \cos(\phi(t) + \frac{\pi}{2}) \cos(\omega_{LOT} + \frac{\pi}{2}) \right) \\
 &= U_{LO} U_{IF} \left(\cos(\phi(t)) \cos(\omega_{LOT}) + \sin(\phi(t)) \sin(\omega_{LOT}) \right)
 \end{aligned} \tag{2}$$

When inserting I and Q into the first equation the second term can be rewritten using $\cos(x + \frac{\pi}{2}) = -\sin(x)$. The last equation is the definition of the trigonometric addition theorem and yields:

$$U_{RF}(t) = U_{LO} U_{IF} \cos(\omega_{LOT} + \phi(t)) \tag{3}$$

As can be seen from (2) and (3) only one sideband passes through the mixer as the other one is cancelled. By providing appropriate inputs to I and Q with $\phi(t) = \omega_{IFT}t + \Phi$ a single RF output signal results and both the frequency and phase (Φ) can be controlled:

$$U_{RF}(t) = U_{LO} U_{IF} \cos((\omega_{LO} + \omega_{IF})t + \Phi) \tag{4}$$

The added complexity in the system compared to a single balanced mixer introduces new deviations examined below.

The first thing to consider is the splitting of the LO signal and the combining of the two halves of the RF signal to form the final RF signal. An unequal splitting of LO enhances any imbalance of the two mixers and leads to an image sideband feed-through, and likewise an unequal addition in the last process of the IQ mixer gives a larger LO feed-through. Also the mixers themselves may have a different response and unmatched non-linear behaviour to the input signals.

Additionally, the 90° -phase-shift before LO_2 for the quadrature mixer may not be exact, which will shift the two signals and disturb the cancellation of the sideband.

It is common to add the following characteristic values to the ones in the previous subsection to describe an IQ mixer in a datasheet:

image rejection (dB)

This describes the ratio of the image sideband to the desired sideband output. The bigger the rejection the better the image sideband suppression.

IQ amplitude deviation (dB)

A measure of how differently the two mixers connected to I and Q respond to the same IF input signal in amplitude. A smaller deviation means a better balanced mixer.

IQ quadrature phase deviation (deg)

A measure of how much the two mixers connected to the I and Q port deviate in phase from the ideal 90°. A smaller value gives a better cancellation of the sideband.

As seen in this section there are many possible sources of deviations that can interact, adding up or diminishing each other. A mathematical model to include each one as a distinct term would be overly complex and would provide no real advantage regarding the calibration of such a mixer. However a simpler mathematical model is useful as a quantitative description of the signal processing of a real IQ mixer.

It is more sensible to generalize the possible deviations into groups and formulate an expression that describes the RF output from an input signals $I(t)$, $Q(t)$ and $U_{\text{LO}}(t)$ over a specified inputrange:

$$U_{\text{RF}}(t) = \sum_i^{\infty} a_i I^i(t) \sum_j^{\infty} a_j U_{\text{LO}}^j \cos^j(\omega_{\text{LO}} t) + \sum_k^{\infty} a_k Q^k(t) \sum_l^{\infty} a_l U_{\text{LO}}^l \cos^l(\omega_{\text{LO}} t + \Phi) \quad (5)$$

In (5) the mixing process is written in a general form. It is easy to see the non-linear behaviour of the mixer in all three signals $I(t)$, $Q(t)$ and $U_{\text{LO}}(t)$. For computational purposes the sum can be truncated to some finite polynomial.

3 Calibration

In this section a robust calibration procedure is presented. The aim is to allow the prediction of exact I and Q signal required to produce a specific RF output. First the necessary setup is described. The vector network analyser (VNA) and arbitrary waveform generator (AWG) are introduced followed by the limitations of this setup and what deviations it is able to correct. The calibration procedure is then presented in detail.

3.1 Calibration setup and calibration model

The calibration setup is shown in figure 5. It consist of an Agilent E5071C ENA Series Network Analyser (VNA) and a Tektronix AWG 5014C Arbitrary Waveform Generator

(AWG) connected to the Mini Circuits IQ-0307LXP IQ mixer using four FlexTest CBL-5FT-SMSM+ cables. Port1 of the VNA is connected to the LO port of the mixer and port2 to the RF port. The I and Q signals are provided by an AWG on the channels CH1 and CH2.

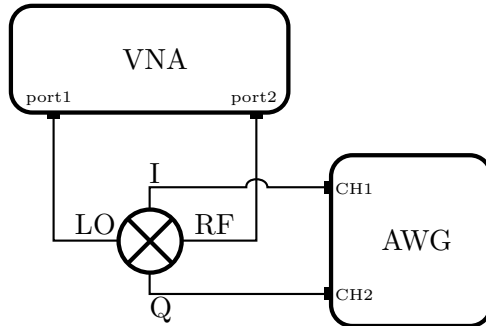


Figure 5: The calibration setup

The VNA can measure the transmission or reflection coefficient over a frequency range up to 20GHz. In this setup the VNA provides a fixed set power (10dBm) while sweeping the frequency at port1 and measures the voltage amplitude U and phase-shift ϕ of the RF signal at port2. These values can be represented as a complex number $Ue^{i\phi}$, from which the real and imaginary part can be obtained.

The I and Q input signals are generated by the AWG. The AWG is capable of producing arbitrary waveforms by stepping through a list of amplitude values. It can produce waveforms in a loop by running through values sequentially or step through many waveforms in a complex sequence independently for each channel. In the calibration process only the offset voltage capability of the AWG for CH1 and CH2 is used to step through a range of DC values for I and Q.

Not all types of errors will be corrected by this calibration. Since the RF output on port2 of the VNA is measured only over a narrow bandwidth centered on the sweeping frequency at port1 and so variations of the RF signal such as its skewness due to higher harmonics will not be detectable. Only mean values of the deviations are provided at any given frequency for the phase and magnitude of the RF output.

A second point to consider is the use of DC values as I and Q signals. The response of the mixer for sinusoidal IF, I and Q signals is not identical to the DC response, since no frequency dependent behaviour can be examined or corrected for such as intermodulation products with the IF frequency and bandwidth limiting factors for higher IF frequencies introduced by cables and instruments.

Since the IF signal frequencies used in this thesis are typically much smaller than the final RF output this deviations are neglected so far. A more advanced examination of the RF response to I and Q might also include different sinusoidal signals with varying frequency. This additional data could be implemented as a frequency dependent correction to the calibration data obtained for DC values.

A good way to visualise the distortions that are able to be corrected with this calibration is

an IQ plot, where the I signal is plotted on the x - and the Q signal on the y -axis. Subject to the limitations discussed above the dashed lines in the IQ plot represented by figure 6 trace out the necessary trajectory through IQ space required to generate an ideal RF signal without distortions for some fixed LO signal.

The I and Q signal for an ideal mixer would be represented by a circle in the IQ plot with $I = A \cos \omega_{\text{IFT}} t$ and $Q = -A \sin \omega_{\text{IFT}} t$. An amplitude imbalance between the I and Q mixer can be corrected by a scaling factor for one axis, or both if the global signal strength must be increased.

The example shown for the I signal corrects for a amplitude imbalance. The I component is drawn with a smaller amplitude than the one from the ideal trace. Since this IQ plot represents the required signal to generate an ideal RF output, this correspond to a I signal which is too strong and is scaled down.

A global phase shift error between I and Q can be corrected by a rotation of the coordinate system. To visualize the change in the phase, the I component is additionally scaled down.

A DC offset on either channel can be corrected by shifting the trace along the appropriate axis, in this case the I axis.

The final possible correction concerns non-linear behaviour for DC I and Q signals. Amplitude dependent non-linearities result in a warping of the ideal circle. Using a polynomial model of higher order in I and Q allows higher order non-linearities to be corrected as well.

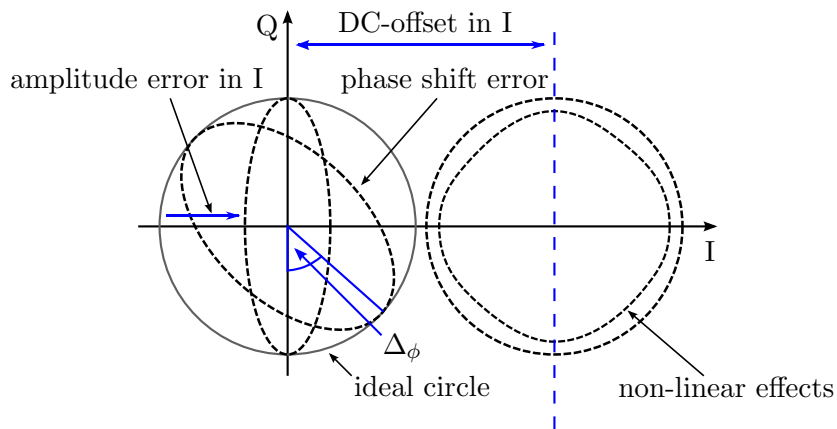


Figure 6: The influence of non-ideal behaviour on the signals I and Q in an IQ plot. The non-linear effects error has an additional DC offset. Adapted from [13]

A model describing these four corrections would be:

$$I(t) = a_0 + a_1 A \cos(\omega_{\text{LO}} t) + a_2 A^2 \cos^2(\omega_{\text{LO}} t) + \dots \quad (6)$$

$$Q(t) = b_0 + b_1 A \sin(\omega_{\text{LO}} t + \Delta_\phi) + b_2 A^2 \sin^2(\omega_{\text{LO}} t + \Delta_\phi) + \dots \quad (7)$$

Here a_0 and b_0 correct DC offsets, while a_1 and b_1 are the necessary amplitude factors for a balanced output. Δ_ϕ corrects the phase shift according to figure 6. Finally, the additional terms $a_n A^n \cos^n(\omega_{\text{LO}} t)$ and $b_n A^n \sin^n(\omega_{\text{LO}} t + \Delta_\phi)$ correct for non-linearities, up to order n .

3.2 Calibration procedure

Using the above model this subsection details the steps required to obtain calibration data and derive calibration parameters. Then the process of generating calibrated I and Q inputs is presented. The implementation of these steps in MATLAB® and the integration into the software package Pulsecontrol is discussed in the second part.

3.2.1 Calibration steps

To calibrate the IQ mixer a DC voltage grid pattern in I and Q is stepped through and the RF response for several LO frequencies is measured on the VNA. The range of the grid gives the maximum obtainable RF response amplitude and the number of grid points determines the accuracy of the calibration. For every I and Q value the VNA performs a frequency sweep with constant output power at port1 and measures the response on port2. Thus the real and imaginary part of the RF response can be written down as a function of DC I and Q for the LO frequency as a parameter: $\text{Re}_{\omega_{\text{LO}}}(I, Q)$, $\text{Im}_{\omega_{\text{LO}}}(I, Q)$.

For a uniformly relation of real and imaginary part with I and Q this relationship can be inverted. The new function is: $I_{\omega_{\text{LO}}}(\text{Re}, \text{Im})$, $Q_{\omega_{\text{LO}}}(\text{Re}, \text{Im})$. As stated before this process is only possible for a uniform function. Very strong non-linear effects can corrupt the calibration. It is necessary to visually examine the data at least for the start and end LO frequencies in the calibration set. In the next section detailing the calibration results, figure 7a represents a measurement with such non-linear effects at the edges.

The discrete measurement values are now fitted using the method of least square to a two dimensional polynomial. The algorithm uses matrix operations based on Singular value decomposition [14] and is implemented³ in MATLAB®. The model is of the form:

$$Y(x, y) = a_{00} + a_{01}y + \dots + a_{0N}y^N + a_{10}x + a_{11}xy + \dots + a_{1,N-1}xy^{N-1} + \dots + a_{N0}x^N \quad (8)$$

³2D polynomial fitting with SVD by Richard Whitehead, <http://www.mathworks.de/matlabcentral/fileexchange/31636-2d-polynomial-fitting-with-svd>

$Y(x, y)$ now yields a parametrisation of I and Q over the complex plane for a single LO frequency. By inputting the desired RF output signal $U_{\text{RF}}(t) = U_0 e^{i(\omega_{\text{IF}} t + \phi)}$ with $\omega_{\text{IF}} = \omega_{\text{RF}} - \omega_{\text{LO}}$ as the IF frequency into the parametrisation, the calibrated values for I and Q that would produce this output can be obtained. Thus a calibration set consists of a number of coefficients for every measured LO frequency.

The result of the calibration can be improved by selecting only the data points within a circular region $\text{Re}^2 + \text{Im}^2 \leq R^2$ in the complex plain. Using this approach non-linear behaviour may be excluded. R represents now the maximum amplitude of the RF signal that can be produced. Increasing U_0 beyond this region while using polynomials of higher order may produce I and Q signals outside of the mixer's maximum ratings.

The order N of the polynomial used in the fit can be adjusted to minimize residuals. Increasing the order beyond a critical value may decrease the quality of the overall fit. This behaviour is described by Runge's Phenomenon[15] for one dimension and equally distanced points. It concludes that higher order polynomials can lead to oscillations at the edge of the chosen interval for the fit. The same basic principle applies for the two dimensional fit of high order to the masked calibration data.

A possible improvement is to use a spline-fit, based on piecewise polynomial with smooth matching conditions. Since a piecewise polynomial for spline creation use small orders, the data could be fitted, without oscillations at the borders.

3.2.2 Implementation

Safe values for the calibration of the mixer are chosen within the maximum ratings of the datasheet. In case of the IQ-0307LXP the maximum input power is +26dBm shared across all inputs. The power of the LO signal is set to +10dBm, which is at the bottom of the drive level specified. The remaining $+(2 \cdot 8)\text{dBm}$ gives the maximum power that may be input to the I and Q ports. The maximum range for a square grid in I and Q is then:

$$\begin{aligned} P &= \frac{10^{\frac{8\text{dBm}}{10}}}{1000} \\ U_{\text{RMS}} &= \sqrt{PR} \\ U_{\text{P}} &= \sqrt{2PR} \quad , R = 50\Omega \\ &\approx 0.80 \text{ V} \end{aligned}$$

A lower value of ± 0.5 within the maximum rating is chosen for the range, since non-linear effects limit the usable RF amplitude (figure 7a) at the lower LO frequency limit and a bigger range would yield no additional information. To obtain detailed data the grid is stepped through in 101x101 points. The LO frequency range of the mixer is 3-7GHz. This calibration only examines the three frequencies 3GHz, 5GHz and 7GHz to compare the behaviour at the centre with the upper and lower limits. The data at the limits is expected to contain more non-linear distortions.

The specification of the grid size and number of LO frequencies has a big run-time impact on the calibration. Only three values for the LO frequencies are chosen, to minimize run-time and any external effects on the measurement.

The configuration of the calibration is saved into a data structure inside MATLAB[®] called a `scan`. The software package Special Measure developed by Hendrik Bluhm et al.⁴ uses this scan structure to perform a measurement via the function `smrunt()`. Special Measure is a set of scripts for MATLAB[®] to control instruments and automate measurement tasks. Here it controls the VNA and AWG and is used for data acquisition. The operation of Special Measure is beyond the scope of this thesis.

Special Measure is not used directly but is called by `calrun()`. This function defines a standardized way of running arbitrary calibrations and simulations in a Special Measure context.

A calibration is defined as a standardized structure, shared between different kinds calibration tasks, which is then processed by `calrun()`. `calrun()` starts a measurement via Special Measure and defined by `scan` and saves the result as two 3d arrays for the real and imaginary part of the VNA output into a file. This data is then processed by an analysing function `fitRiData()`, which fits the model (8) to the data and obtains the coefficients for every LO frequency as a calibration set. The order of the polynomial and the radius used to mask are parameters of this function. `calrun()` can be executed several times using the same measurement data to optimize the degree and radius.

The measured data and resulting model can be evaluated by the function `plotRiData()`. It is useful to examine the $I_{\omega_{\text{LO}}}$ (Re, Im) and $Q_{\omega_{\text{LO}}}$ (Re, Im) representation to check whether the data is uniformly and thus usable for a calibration. The radius of the mask and order of the polynomial, can than be adjusted and the analysis of the data repeated to obtain optimal results.

For the IQ-0307LXP and this input values a polynomial of order 4 and a mask radius of 0.1V are chosen.

The calibration set created in `calrun` is saved in a global structure `caldata` and can now be used to create calibrated RF pulses in Pulsecontrol.

Pulsecontrol is not discussed here in detail, since its full functionality is beyond the scope of this thesis. The process of creating and evaluation a calibration using `calrun()` and `plotRiData()` as well as a description of creating RF pulses and chirps with Pulsecontrol can be found in the appendix. Here only the extension of Pulsecontrol to generate RF pulses using calibrated data is described.

Pulsecontrol consists of two part. The first part implements AWG specific functions while the second is a general system for creating and managing pulses in an AWG independent database.

The definition of a pulse can take place at several different abstraction levels. The highest level is the definition of pulse elements characterised by parameters, which implement

⁴Special Measure is a measurement control software designed to provide a simple interface to control instruments and acquire data using MATLAB[®], <http://code.google.com/p/special-measure/>

specific pulse-shapes. Followed by a tabular definition with time-value-pairs. The lowest abstraction level is a simple value list which is executed in the AWG specific atomar time unit. When adding pulses to a AWG the higher level definition are progressively down-converted to a simple value list.

An RF pulses is generated by a new type of top-level pulse element called '`rfpulse`'. By specifying a start and stop RF frequency, the frequency of the LO, the desired RF amplitude, phase and duration the calibration set is used to create calibrated I and Q signals via the function `plsIqFnCreate()`. The function is called inside of the extended `plstotab()`, which is used when converting between abstraction levels.

Beside a RF pulse of a constant frequency a chirp can be generated, when the start and end RF frequencies are not equal.

The results of the calibration of IQ-0307LXP are discussed in the next section. Since the time domain analysis of the RF output signal requires an additional microwave component in the RF signal path depicted in figure 10, the calibration is executed with an directional coupler connected in between mixer and port2 of the VNA, to compensate for the introduced phase offset and attenuation. Since the coupler provides minimal distortions and the phase shift is global compared to I and Q, this introduces only minimal changes in the calibration data.

4 Measurements

In this section the calibration results are evaluated by examining the $I_{f_{LO}}(Re, Im)$ and $Q_{f_{LO}}(Re, Im)$ representation at different LO frequencies and comparing the polynomial fit when repeating the calibrated eleven times. The RF signal of the mixer IQ-0307LXP is analysed in the time domain using an digital serial analyser (DSA). The improvement gained by using calibrated I and Q inputs is compared with simply assuming an ideal mixer with ideal I and Q inputs.

4.1 Calibration results

The calibration shows different mixer behaviour for the three LO frequencies checked, the lower limit, the centre and upper limit of the LO frequency range. Figures 7a, 8a and 9a show the $I_{f_{LO}}(Re, Im)$ and $Q_{f_{LO}}(Re, Im)$ representation of the IQ mixers non-ideal behaviour. The plots show the distortions one would need to apply to the I and Q inputs of an ideal IQ mixer to get the same non-ideal behaviour seen with the mixer being calibrated.

Figure 7a shows pronounced non-linear behaviour at the edge of the IQ range. A small variation in position on the complex plane corresponds to a large change in I or Q voltage. This non-linear behaviour limits the radius of the circular mask to values close to 100mV, while not exceeding the range of acquired data. Figure 7b shows a fourth order model (equ (8)) fit to the data inside the circle marked in figure 7a. Table 1 shows the Root-Mean-Square (RMS) value of the residuals and the maximum absolute residual, representing the maximum error between data and fit. The errors at 3GHz using this model are the most

pronounced, which limits the correction achievable by using this fit compared to 5GHz and 7GHz.

When calibrating solely for a LO frequencies range showing prominent non-linear behaviour, a polynomial of higher order is more suitable. A fourth order polynomial fit was chosen as a compromise between minimizing the number of coefficients to store for every LO frequency and minimizing the residual RMS values at the centre frequency, without producing oscillations near the limits of the fitting range by increasing the order. The oscillations for high order polynomials are described by Runge's Phenomenon[15] discussed previously. This oscillations may increase the maximum residuals.

To examine the evolution of the coefficients over time the calibration is repeated 11 times (figure 7c). Run #1 is recorded immediately after turning on the mixer. Runs #2-11 are recorded in sequence, starting one hour after turning on the power. The total time for one calibration run is around 26 minutes.

Figure 7c shows no significant variation of the coefficients between runs. For a LO input of 3GHz higher some of the higher order coefficients are large, indicating strong non-linear effects. These coefficient values are consistent over the eleven runs, which suggests reproducible behaviour of the calibrated mixer.

Figure 8 shows the calibration results for a LO input of 5GHz. The I and Q plots show a more linear behaviour than at 3GHz. The variation of the coefficients (figure 8c) is fluctuating in a narrow region, which is consistent with figure 7c.

Similar behaviour is seen for the data at 7GHz (figure 9c), with the exception of run #1, which differs from the subsequent runs. As previously (section 3.2.1) discussed for every I and Q voltage pair the RF response is measured at the examined LO frequencies, e.g at (I_0, Q_0) using 3GHz, 5GHz and 7GHz as LO frequency, followed by (I_1, Q_0) at 3GHz, 5GHz and 7GHz and subsequent acquisitions. Thus the deviation at 7GHz is unexpected, since at 3GHz and 5GHz LO frequency run #1 is not exhibiting this behaviour.

Once the mixer is warmed up the calibrations are interchangeable and data from run #11 is chosen to compare the calibrated and uncalibrated mixer by analysing the time domain signal.

	3GHz	5GHz	7GHz
RMS residuals I (mV)	14.38	0.40	0.37
RMS residuals Q (mV)	21.40	0.09	0.47
Max. residuals I (mV)	63.97	9.74	9.62
Max. residuals Q (mV)	120.65	0.31	3.08

Table 1: Goodness of fit based on the residual RMS and maximum deviation of the fit model to the data for different LO frequencies.

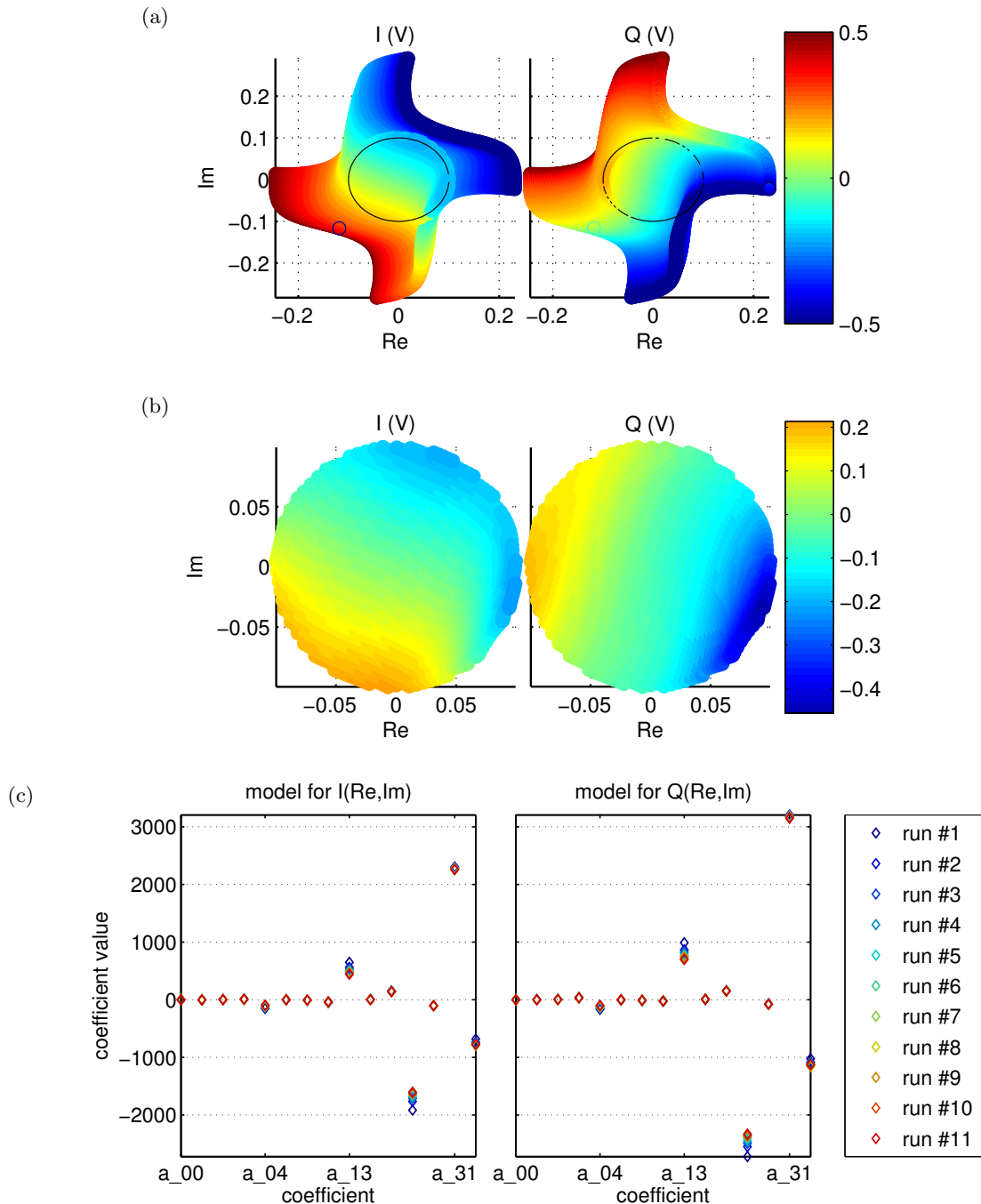


Figure 7: Calibration data and calibration model at 3GHz LO frequency. (a) is the calibration data with the fit mask indicated by the circled region. (b) is the fit inside the masked region. (c) is the evolution of the coefficients for 11 consecutive runs.

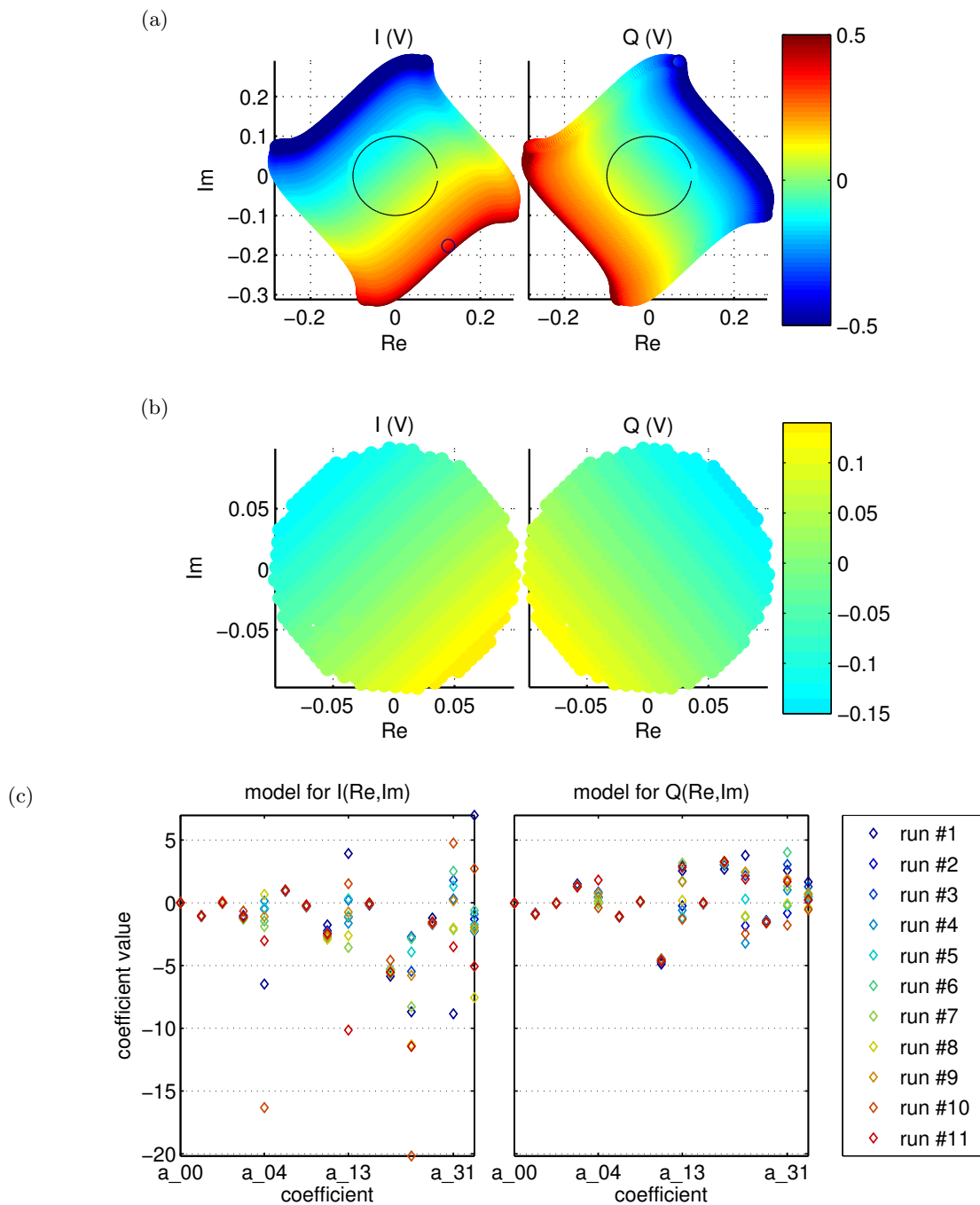


Figure 8: Calibration data and calibration model at 5GHz LO frequency. (a) is the calibration data with the fit mask indicated by the circled region. (b) is the fit inside the masked region. (c) is the evolution of the coefficients for 11 consecutive runs.

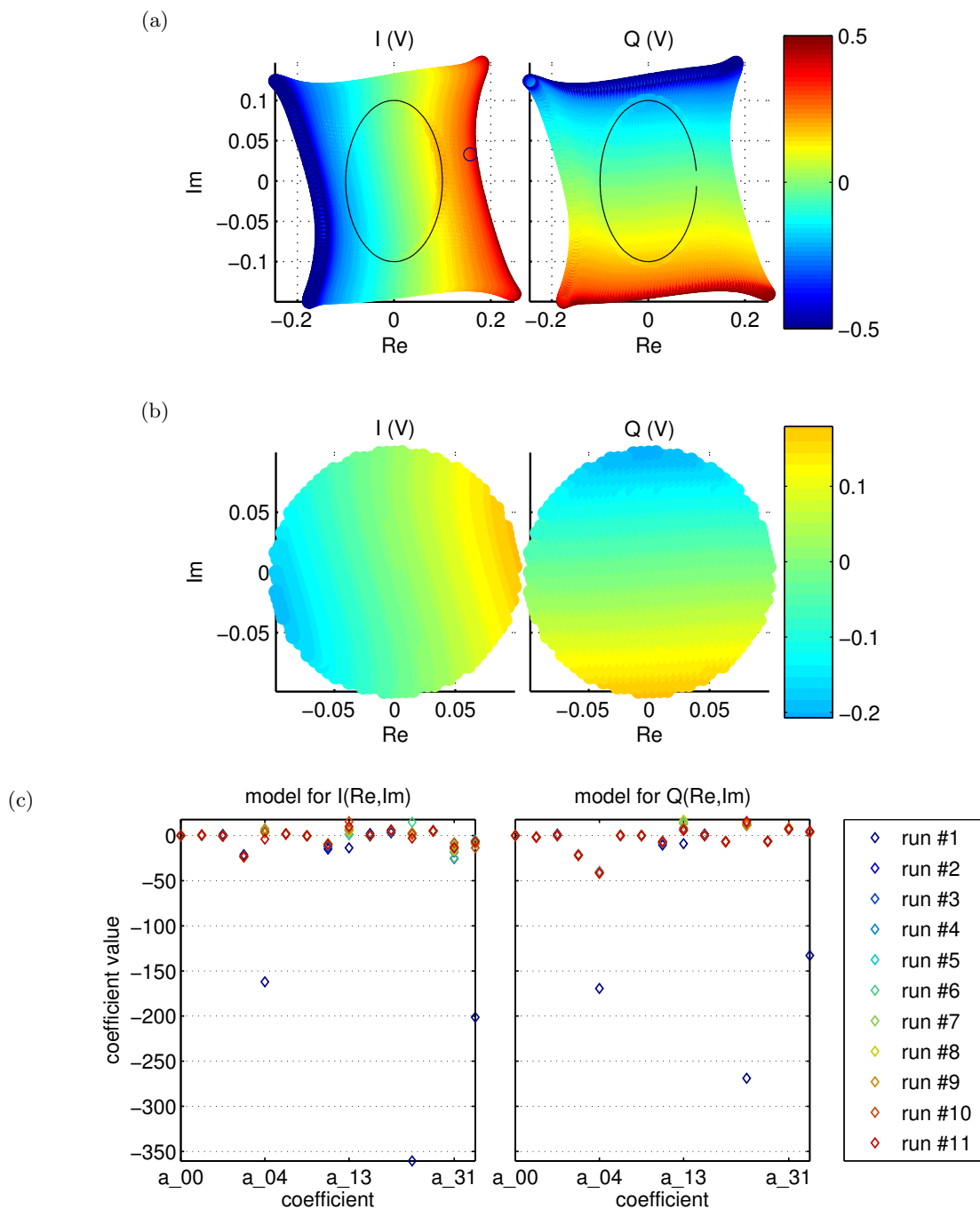


Figure 9: Calibration data and calibration model at 7GHz LO frequency. (a) is the calibration data with the fit mask indicated by the circled region. (b) is the fit inside the masked region. (c) is the evolution of the coefficients for 11 consecutive runs.

4.2 Comparison of calibrated and uncalibrated mixer

The RF signal of the mixer is measured using a Tektronix Digital Serial Analyzer DSA 820 in sampling mode. The DSA requires an external trigger signal to synchronise the sampling process. The measuring equipment setup is shown in figure 10. Port1 of the VNA is supplying the LO signal at 10dBm as before. I and Q are supplied by the AWG. The DSA is connected through the directional coupler C20-0R520 from Marki Microwave to the RF port of the mixer. The coupler passes the RF signal to the DSA with minimal distortion. Connected to the weakly coupled (-20dB) port of the coupler is a wideband amplifier ZVA-183-S+ from Mini Circuits, which provides a signal with sufficient amplitude for the external trigger of the DSA.

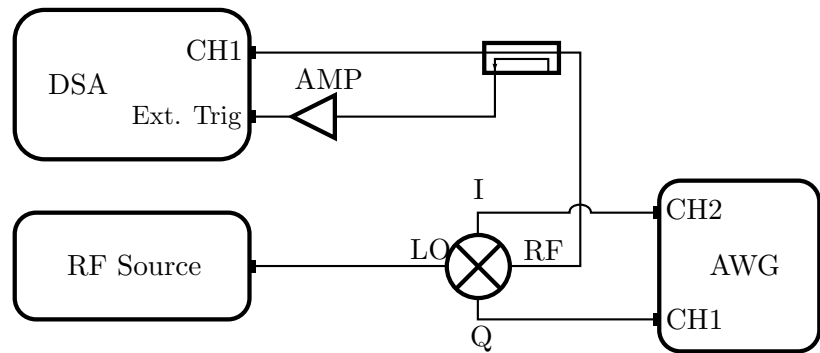


Figure 10: The measurement setup to measure the RF signal in the time domain using a DSA 820. The sampling is controlled by the external trigger source connected via the ZVA-183-S+ amplifier to the C20-0R520 coupler.

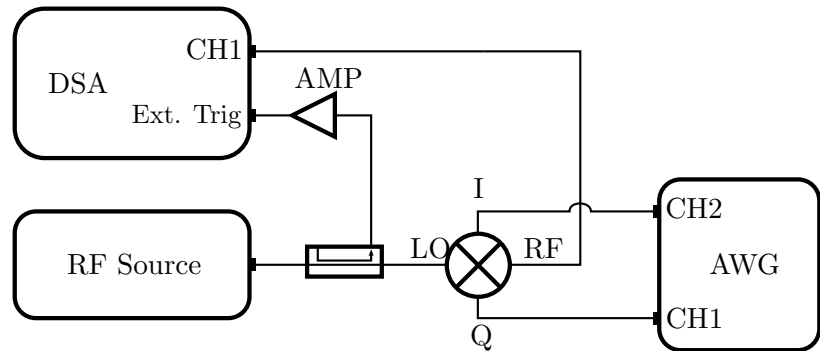


Figure 11: The measurement setup to measure the phase of the RF signal.

To measure the phase shift introduced by the IQ mixer the setup is modified as shown by figure 11. The directional coupler is moved on the RF source output. The phase shift given by DC I and Q signals can now be measured. It is not possible to measure the phase shift with a non-DC I and Q in this setup.

The DSA time resolution is set to a number which will record 10 periods of the RF signal for each LO frequency. The signal is averaged for 10 samples. A sample contains 4000 datapoints.

To obtain the amplitude, frequency and phase of the calibrated and uncalibrated signals a sinusoidal fit of the form:

$$y = a + b \sin(2\pi f + d) \quad (9)$$

is used with a least squares fitting function using Orthogonal-triangular decomposition [16]. The calibrated pulses for the AWG are created using Pulsecontrol and the calibrated data previously obtained. They are compared with ideal signals:

$$I = cA \cos(\omega_{\text{IFT}} t + \phi)$$

$$Q = -cA \sin(\omega_{\text{IFT}} t + \phi)$$

where c is a factor to correct for the conversion loss obtained from the datasheet. The datasheet states a typical conversion loss of -5.5dB. Therefore the amplitude is expected to be reduced by $c = 10^{\frac{5.5}{20}} \approx 1.884$.

4.2.1 Crosstalk

Figure 12 shows the RF output signal at three LO frequencies with nominal zero I and Q inputs. In each plot I and Q are set to ground (blue) and calibration corrected 'ground' (red). For 3GHz (figure 12a) the uncalibrated blue curve shows a distinct imbalance between two phase shifted sinusoidal signals. The calibrated red curve improves this situation and the amplitude is reduced due to the improved cancelling of the two components of the crosstalk signals. The same is true with 7GHz as the LO frequency (figure 12c). For the 5GHz LO frequency (figure 12b) the mixer is already well balanced and the calibrated gives little improvement.

	not calibrated	calibrated	datasheet typ.
3GHz	31	40	30
5GHz	38	41	30
7GHz	43	52	30

Table 2: Comparison of LO-RF isolation for 10dBm LO signal power and different LO frequencies. Values in (-dB).

Table 2 shows the LO-RF isolation obtained presented by comparing the LO signal power of 10dBm with the peak-to-peak values V_{PP} of the RF signal from the data plotted in figure 12. Voltage values are converted into dBm and the attenuation with respect to the LO power is listed. The isolation is always better than the typical value given in the datasheet. The uncalibration increases the isolation by additional 9dB compared to the uncalibrated case for the three measured LO frequencies.

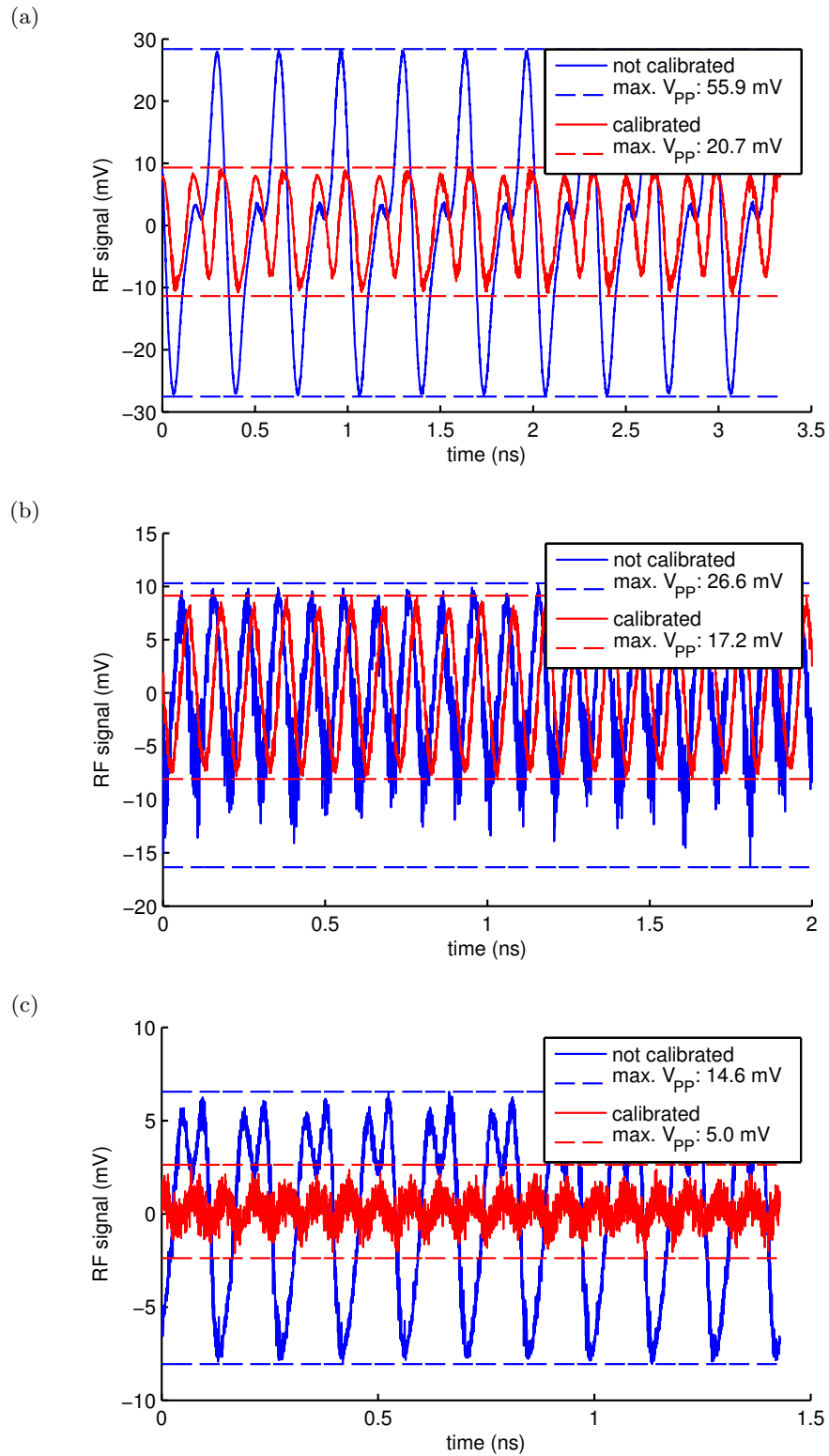


Figure 12: The crosstalk when I and Q are set to ground with and without calibration corrections. (a) is the crosstalk at 3GHz, (b) at 5GHz and (c) at 7GHz

4.2.2 Amplitude

This section compares the linearity of set versus obtained amplitude in the calibrated and uncalibrated case for a 25MHz frequency shifted RF signal. An amplitude sweep is performed with 20 datapoints from 5mV to 100mV. Figures 13-15 show the RF output signal.

Figure 13a shows the data obtained from the DSA for a LO input of 3GHz. For small amplitudes the LO crosstalk is the dominant signal, followed by a transition region where the LO crosstalk is comparable to the frequency shifted RF output signal generated by I and Q and finally at larger powers there is a linear dependence of set versus measured amplitude. The transition region is shifted to smaller amplitudes when calibrated, since the crosstalk is reduced as discussed above.

The set versus measured amplitude is plotted in figure 13b. The measured RF amplitude comes from fitting to equation (9). Data marked with a '*' is excluded from the linear fit (solid line).

The calibrated data shows a variation from the expected unity gradient. At 25MHz there is no significant improvement of the calibration to the uncalibrated case in relation to the amplitude behaviour. As the LO frequency goes up, the crosstalk goes down and the difference of the blue and red gradient decreases for 5GHz (figure 14b) and 7GHz LO frequency (figure 14b).

This shows the limitation of the calibration model used here. Since only DC values of I and Q are used to deduce the behaviour of the mixer also for non-DC signals the calibration is only valid for slow varying I and Q signals.

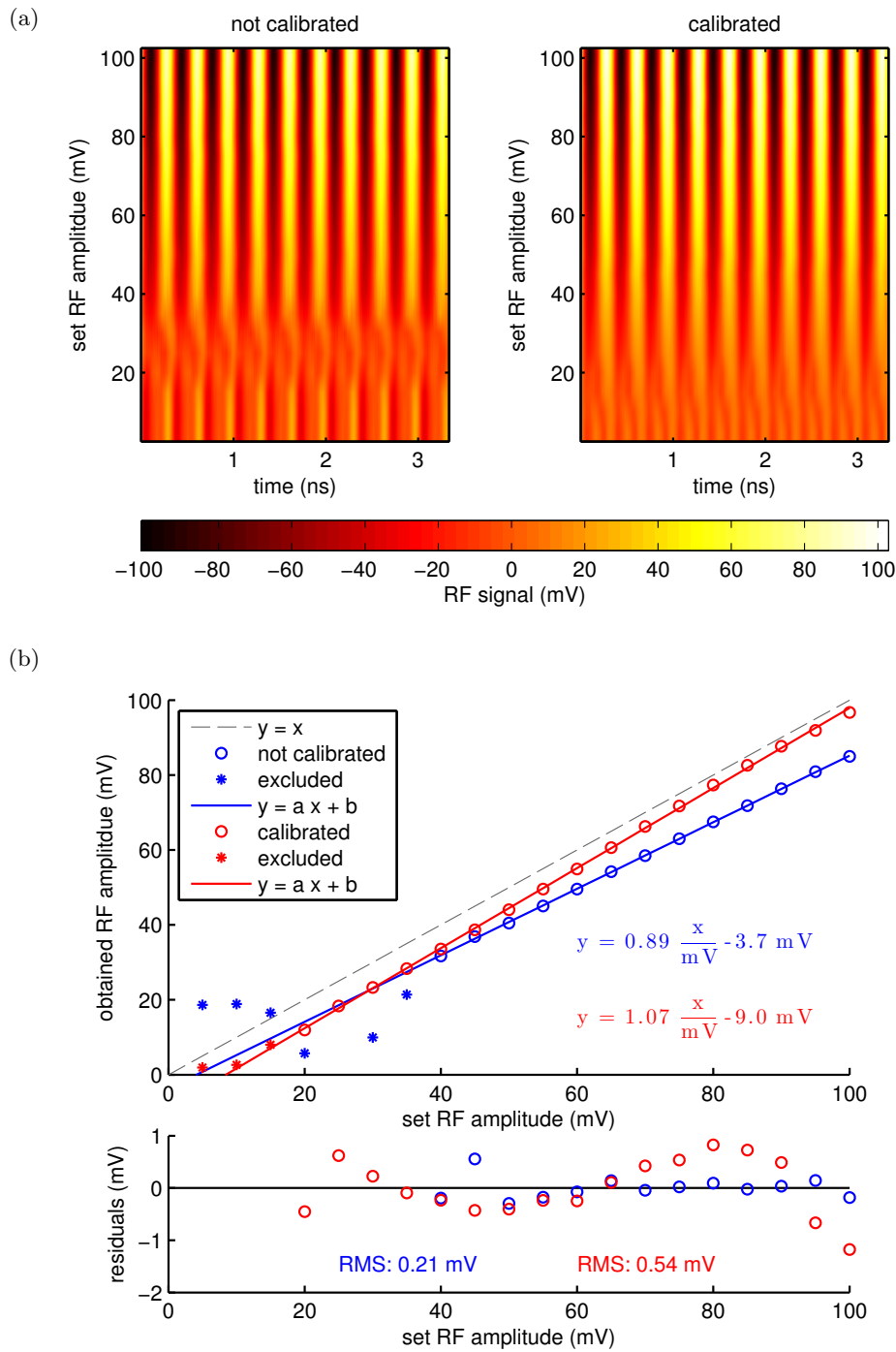


Figure 13: The set versus the measured amplitude at 3GHz LO frequency and 25MHz IF frequency. (a) is a image plot with transition from crosstalk to signal. (b) is a linear fit of the amplitude

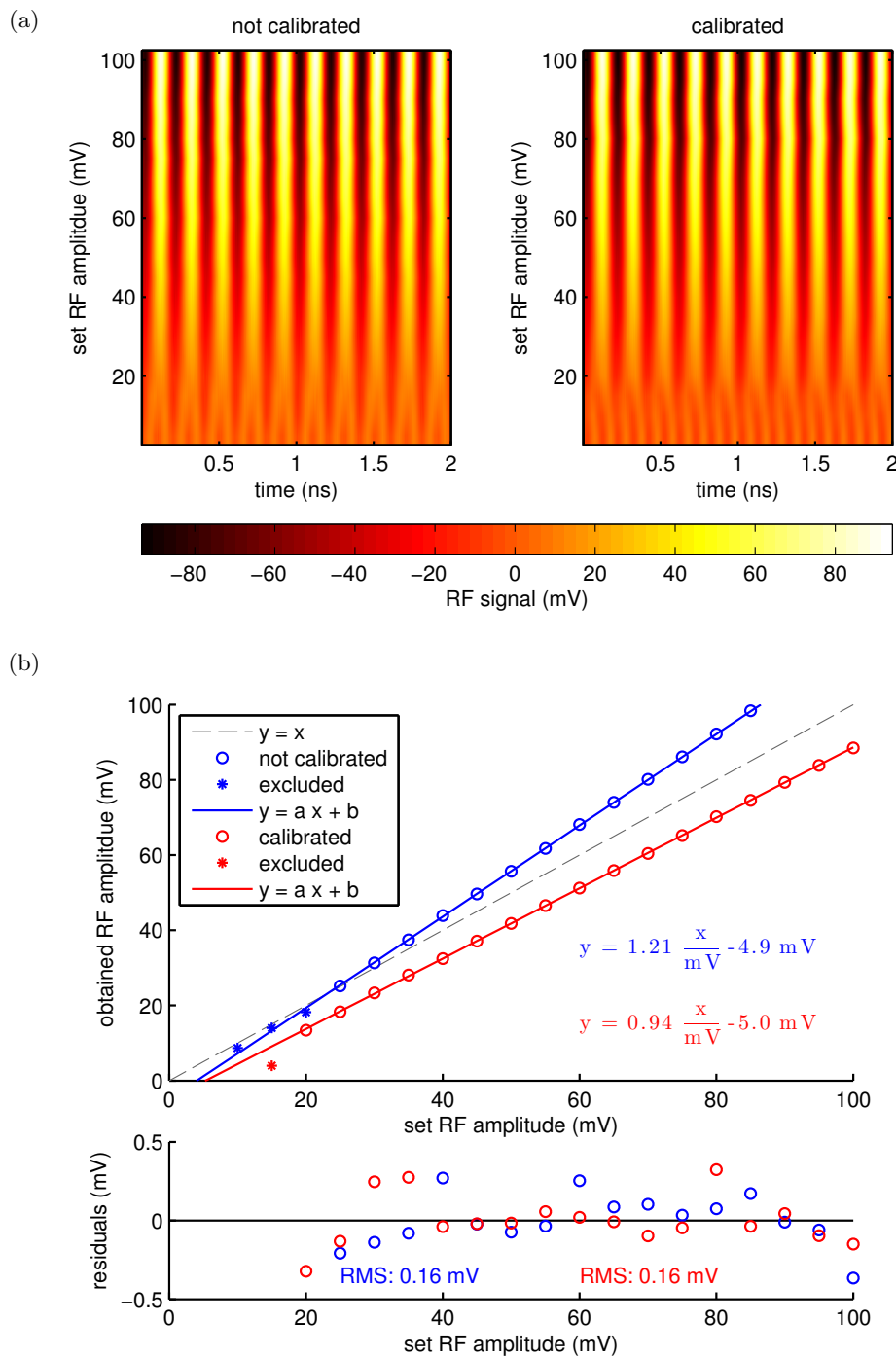


Figure 14: The set versus the measured amplitude at 5GHz LO frequency and 25MHz IF frequency. (a) is a image plot with transition from crosstalk to signal. (b) is a linear fit of the amplitude

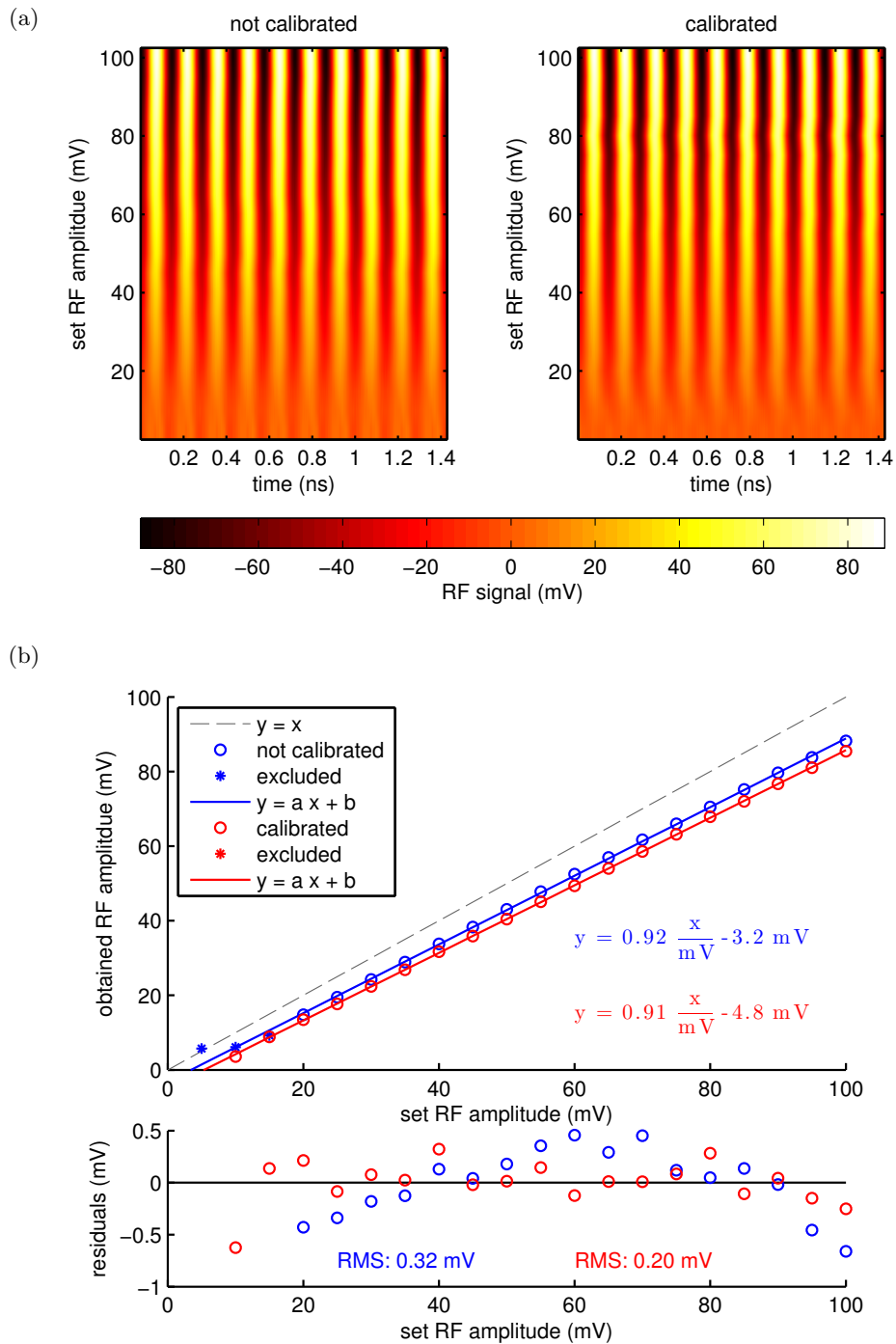


Figure 15: The set versus the measured amplitude at 7GHz LO frequency and 25MHz IF frequency. (a) is a image plot with transition from crosstalk to signal. (b) is a linear fit of the amplitude

4.2.3 Frequency

The frequency behaviour is examined by a frequency sweep from $f_{LO} - 45\text{MHz}$ to $f_{LO} + 50\text{MHz}$ in 20 steps. The amplitude is set to a fixed value of 100mV.

Figure 16a, 16b and 17 show the set versus the measured frequencies at 3GHz, 5GHz, and 7GHz LO input. Additionally the RF amplitude versus the set frequency is plotted to examine the amplitude response at different frequencies.

The frequency behaviour of the uncalibrated mixer is linear and has the expected slope of one, but a varying amplitude. The calibrated case adjusts the amplitude. This improves the amplitude response for 3GHz (figure 16a) and 5GHz (figure 16b). At 7GHz LO frequency (figure 17) the calibration has no noticeable effect on the amplitude.

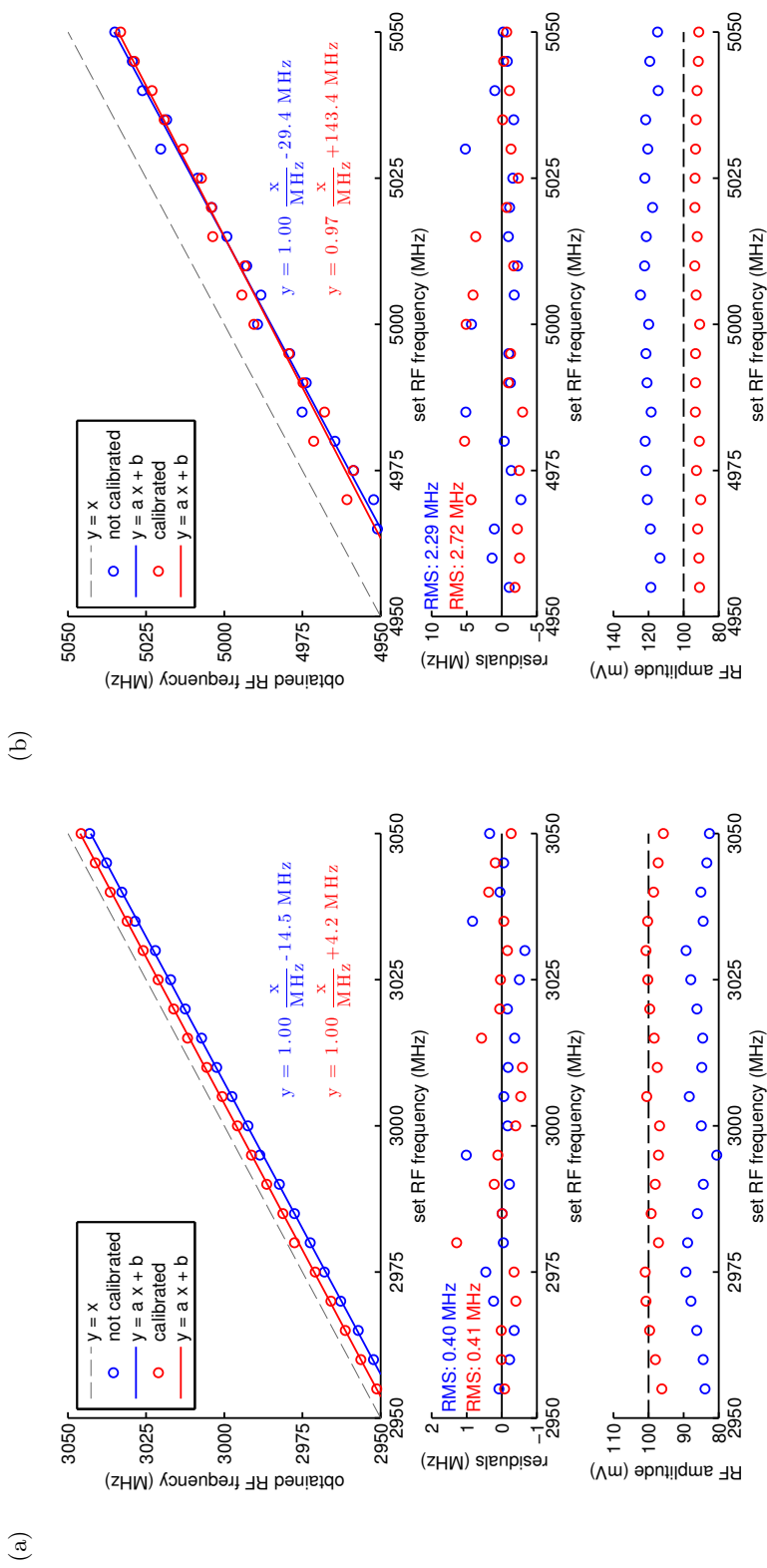


Figure 16: The set versus the measured amplitude at 3GHz (a) and 5GHz (b) LO frequency and 25MHz IF frequency.

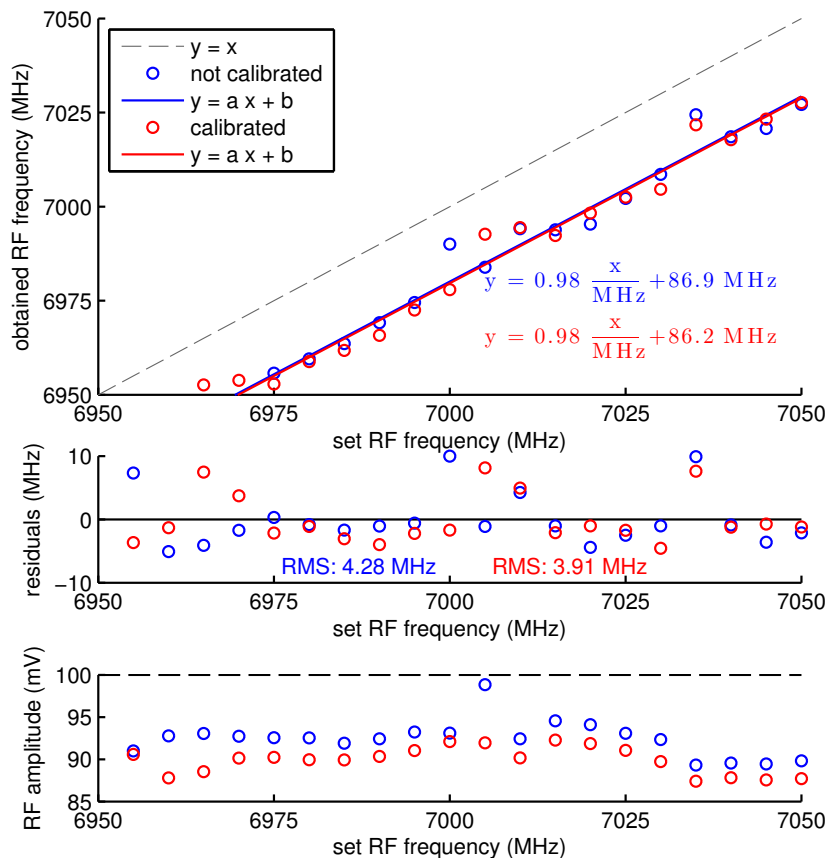


Figure 17: The set versus the measured frequency at 7GHz LO frequency and 100mV RF amplitude.

4.2.4 Phase

The phase is measured by reconfiguring the measurement setup as shown in figure 11. Only DC values for I and Q can be used, since the phase relation between a varying I and Q signal from the AWG and the VNA would be undefined so synchronising the sampling of data by the DSA would be impossible. The phase-shift behaviour at non-zero frequencies is assumed to be comparable to the DC case within the tolerance of the frequency behaviour discussed above.

The phase behaviour of the IQ mixer is examined by a phase shift sweep from -162° to 180° in 20 steps. The RF amplitude is set to a fixed value of 100mV.

Figure 18a, 18b and 19 show the set versus the measured phase. Additionally the RF amplitude versus the set phase is plotted to view the amplitude response at different phase shift values. Since only DC I and Q values are used, as in the calibration measurement, the calibrated case is expected to vary mostly within the errors of the fit from table 1 from the ideal case.

The phase behaviour of the not calibrated mixer is linear and has the expected slope of one, but a varying amplitude. The calibrated case adjusts the amplitude. This improves the amplitude response for 3GHz (figure 18a) and especially 5GHz (figure 18b), for which the calibration model has the smallest residuals compared to the other LO frequencies. At 7GHz LO frequency (figure 19) the calibration produces an amplitude systematically lower than expected, but the variations in amplitude are decreased.

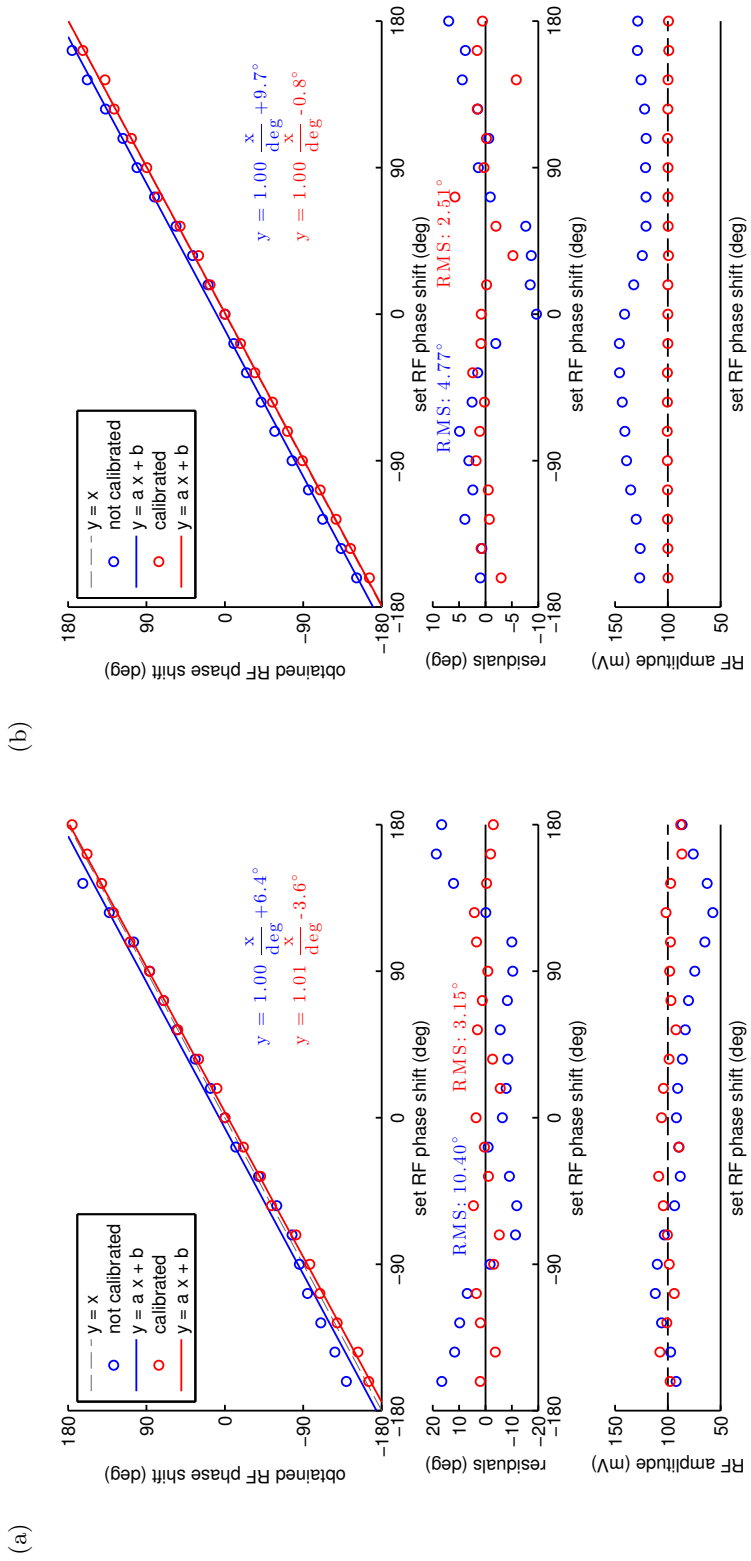


Figure 18: The set versus the measured phase shift at 3GHz (a) and 5GHz (b) LO frequency and 100mV RF amplitude.

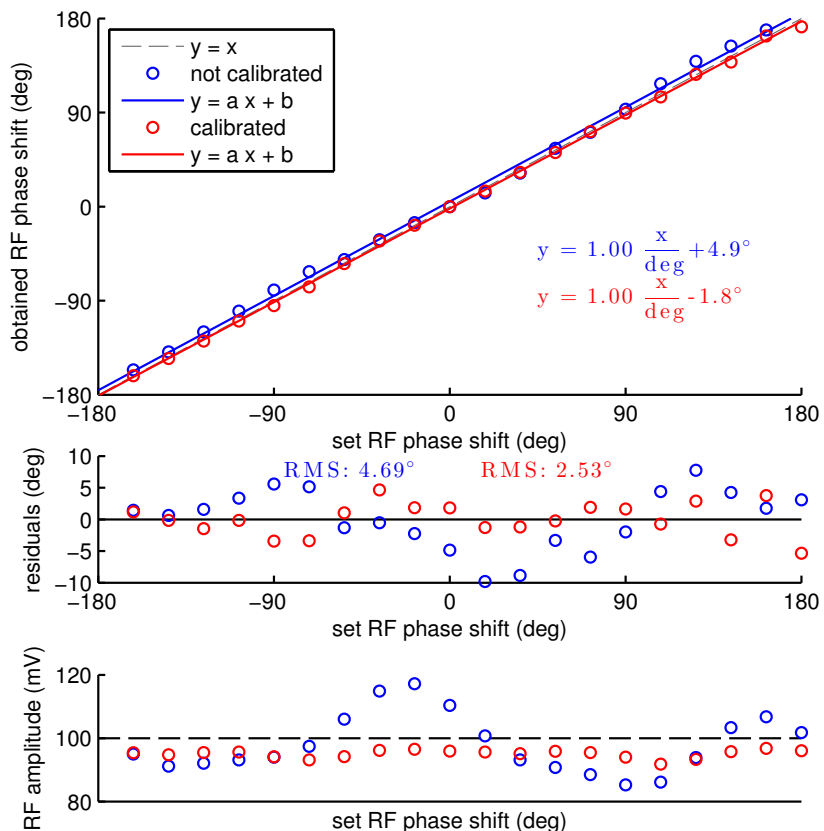


Figure 19: The set vs. the measured phase shift at 7GHz LO frequency and 100mV RF amplitude in relation to the 0° phase.

5 Conclusion

The assembly and calibration of a RF vector source using an IQ mixer, a Vector Network Analyser and an Arbitrary Waveform Generator was successful. The functionality to create RF pulses adjustable in amplitude, frequency and phase, as well as chirps was implemented into Pulsecontrol. Since the IQ mixer calibration procedure was based on traversing a DC grid in I and Q it has no significant improvement over the not calibrated mixer at 25MHz IF frequency in an amplitude sweep or an IF frequency sweep from -45MHz to 50MHz. However the DC properties were improved: The crosstalk was reduced by 9dB compared to the uncalibrated mixer, which enables the operation of the mixer at IF frequencies and low amplitudes, where otherwise crosstalk would disturb the signal. The phase sweep with constant amplitude of 100mV shows an improvement in amplitude stability. For the optimal calibrated 5GHz LO frequency the residual RMS value drops 31.7mV to 0.36mV.

The behaviour of the calibrated mixer at non-zero IF frequencies would be improved by weighting the DC calibrated I and Q signals with an IF frequency and amplitude dependent additional function, which could be measured by a calibration run for non-zero IF frequencies at different amplitudes. A function of the form $y(x) = a(\omega_{IF}) + b_{\omega_{IF}}x + \dots$ may correct the set amplitude and set frequency.

6 Acknowledgments

First and foremost, I would like to thank prof. Hendrik Bluhm for the opportunity to contribute to his work. He was at all times willing to discuss results and give valuable guidance and advice during my project. It was a valuable experience working with modern measurement equipment and radio frequency components.

I also would like to thank the qubit and SQUID group for the warm welcome and support, especially Robert McNeil, who dedicated much time proofreading my thesis and was always ready to help during the course of my work.

In addition, I would also like to thank Tim Botzem for his assistance and the carbon nanoelectronics group for borrowed measurement equipment.

Finally, an honorable mention goes to my family and friends for their understandings and supports on me in completing this work.

List of Figures

1	Simple single-ended mixer.	7
2	Double balanced mixer [12]	7
3	Schematic representation of a mixing process	9
4	IQ mixer	11
5	The calibration setup	13
6	The influence of non-ideal behaviour on the signals I and Q in an IQ plot [13].	14
7	Calibration data and calibration model at 3GHz LO frequency.	20
8	Calibration data and calibration model at 5GHz LO frequency.	21
9	Calibration data and calibration model at 7GHz LO frequency.	22
10	The measurement setup to measure the RF signal in the time domain using a DSA 820.	23
11	The measurement setup to measure the phase of the RF signal in the time domain using a DSA 820.	23
12	The crosstalk when I and Q are set to ground with and without calibration corrections.	25
13	The set versus the measured amplitude at 3GHz LO frequency and 25MHz IF frequency.	27
14	The set versus the measured amplitude at 5GHz LO frequency and 25MHz IF frequency.	28
15	The set versus the measured amplitude at 7GHz LO frequency and 25MHz IF frequency.	29
16	The set versus the measured amplitude at 3GHz and 5GHz LO frequency and 25MHz IF frequency.	31
17	The set versus the measured frequency at 7GHz LO frequency and 100mV RF amplitude.	32
18	The set versus the measured phase shift at 3GHz and 5GHz LO frequency and 100mV RF amplitude.	34
19	The set vs. the measured phase shift at 7GHz LO frequency and 100mV RF amplitude in relation to the 0° phase.	35

References

- [1] David P. DiVincenzo. The physical implementation of quantum computation. *Fortschritte der Physik*, 48(9-11):771–783, 2000.
- [2] F. Jelezko R. Laflamme Y. Nakamura C. Monroe Ladd, T. D. and J. L. O'Brien. Quantum computers. *Nature*, 464(7285):45–53, 2010.
- [3] F. A. Zwanenburg, A. S. Dzurak, A. Morello, M. Y. Simmons, L. C. L. Hollenberg, G. Klimeck, S. Rogge, S. N. Coppersmith, and M. A. Eriksson. Silicon Quantum Electronics. *ArXiv e-prints*, June 2012.
- [4] M. Stopa, J. J. Krich, and A. Yacoby. Inhomogeneous Nuclear Spin Flips. *ArXiv e-prints*, May 2009.
- [5] W. Yao and Y. Luo. Feedback control of nuclear hyperfine fields in a double quantum dot. *EPL (Europhysics Letters)*, 92:17008, October 2010.
- [6] D. Mahalu V. Umansky S. Foletti, H. Bluhm and A. Yacoby. Universal quantum control of two-electron spin quantum bits using dynamic nuclear polarization. *Nat Phys*, 5(12):903–908, 2009.
- [7] D. J. Reilly, J. M. Taylor, J. R. Petta, C. M. Marcus, M. P. Hanson, and A. C. Gossard. Suppressing spin qubit dephasing by nuclear state preparation. *Science*, 321(5890):817–821, 2008.
- [8] M. Shafiei, K. C. Nowack, C. Reichl, W. Wegscheider, and L. M. K. Vandersypen. Resolving Spin-Orbit and Hyperfine Mediated Electric Dipole Spin Resonance in a Quantum Dot. *ArXiv e-prints*, July 2012.
- [9] Paul Horowitz and W. Hill. *The Art of Electronics*. Cambridge University Press, 1989.
- [10] Dr. M. Hufschmid. Lecture notes on mixers. Fachhochschule Nordwestschweiz.
- [11] F. S. Goucher, G. L. Pearson, M. Sparks, G. K. Teal, and W. Shockley. Theory and experiment for a germanium $p - n$ junction. *Phys. Rev.*, 81:637–638, Feb 1951.
- [12] H. Bluhm. Lecture notes on high frequency experiments and methodes. RWTH-Aachen, 2011.
- [13] S Sabah and R Lorenz. Design and calibration of iq-mixers. 1998.
- [14] William H. Press, Saul A. Teukolsky, William T. Vetterling, and Brian P. Flannery. *Numerical recipes in C (2nd ed.): the art of scientific computing*. Cambridge University Press, New York, NY, USA, 1992.
- [15] G. Dahlquist and A. Björck. *Numerical Methods*. Dover Books on Mathematics. Dover Publications, 2003.
- [16] Marko Neitola. Four-parameter sinefit from MATLAB® file exchange, 2009.

7 Appendix

7.1 Calibration procedure

After connecting an IQ mixer as in figure 5 the calibration can be conducted using the script `calScript.m`. The script relies on Special Measure, Pulsecontrol and `calrun`, this software bundles need to be present in the MATLAB® search path. The script consists of four parts:

1. the script `smstartup` is called to load the necessary structures and opens connections to the instruments.
 - a) `smdata` is loaded from the mat-file `smdata.mat`, which contains the AWG and VNA instruments and channel definitions. A connection to this two instruments is then established with `smopen()`. `smdata.mat` can be recreated using `smsetup.m`, to change settings like the instruments address, when migrating measurement environments.
 - b) `plsdata` is loaded from the mat-file `awg_pulses/plsdata_iqmx.mat`, which is a pulsedatabase for Pulsecontrol containing a simple pulse with zero amplitude for $1\mu\text{s}$, which loops infinitely called 'zero_loop'. This pulse is used in combination with offset channels, to create DC signals with different voltages on the AWG. To create an empty `plsdata` database and save it to `awg_pulses/plsdata_iqmx.mat` the script `plssetup` can be used. The zero pulse is created inside `pulsedef_iqmx.m` and `pulsegroups_iqmx.m`. Executing this scripts adds it to the empty database. This is not required when `plsdata_iqmx.mat` already exists.
 - c) `awgdata` is loaded from the mat-file `awgdata_{date}.mat` from `pulsegroups_iqmx/` in `awg_pulses/`. The file contains properties of the AWG used. A mat-file can be generated by executing `awgsetup.m`, if not present. The opened AWG connection is assigned to `awgdata.awg`, which is used by Pulsecontrol to communicate with the AWG.
 - d) `caldata` is loaded from the mat-file `caldata.mat`. To create an empty `caldata` structure the script `calsetup.m` can be used.

The final step of `smstartup` is to clear all custom waveforms from the AWG and upload 'zero_pulse'. This pulse is necessary, since only a channel preloaded with a waveform can use offset channels.

2. `scanconfCal` is the definition of a `scan`. By executing this script a structure with the name `scanCal` is created representing the measurement scan. This scan is used by `smrun()` to acquire data for the calibration.

The variables `dcSteps` and `dcMax` in `scanCal` define the steps in which the DC I and DC Q voltage is swepted in a square grid of $(-\text{dcMax} \dots \text{dcMax}) \times (-\text{dcMax} \dots \text{dcMax})$. The LO frequencies, which are measured and the LO signal power are specified with:

```
scanCal.loops(1).rng = [3e9, 7e9]; % from 3GHz to 7GHz
```

```

scanCal.loops(1).npoints = 3; % in three points

scanCal.configfn(4).args{3}[2] = 10; % a LO signal power of 10dBm

```

The **scan** consists of:

a) **scanCal.configfn(:)**

scanCal.configfn(1) sets a trigger for the VNA.

scanCal.configfn(2) instruct the VNA to transmit real and imaginary part of a datapoint.

scanCal.configfn(3) puts the AWG into sequence mode, necessary to select custom pulses by an index (through the channel **pulseLine**).

scanCal.configfn(4) sets port2 as the measurement port on the VNA, sets the LO signal power and selects 'zero_pulse' as the current pulse on the AWG.

scanCal.configfn(5:6) activate CH1 and CH2 of the AWG connected to the I and Q ports of the mixer. The AWG is instructed to execute 'zero_pulse'.

b) **scanCal.loops(1)** initiates a frequency sweep on the VNA.

c) **scanCal.loops(2)** steps through DC I values using channel 'dcI', controlling the offset on CH1. Real and imaginary data is acquired.

d) **scanCal.loops(3)** steps through DC Q values using channel 'dcQ', controlling the offset on CH2.

e) **scanCal.cleanupfn(1)** resets 'dcI' and 'dcQ' to ground level.

3. **caldef_iqmx.m** inside of **caldata_iqmx/** contains the calibration definition used by **calrun()** to run a calibration:

```
clear cal;
```

```

cal.name = 'iqmx_1'; % name of the calibration
cal.log = 1; % saving of calibration results is on
cal.def.dir = 'caldata_iqmx'; % save smrun datafile and cal in caldata_iqmx
cal.def.scan = scanCal; % scan for smrun
cal.def.anafn.fn = @fitRiData; % fitting function
cal.def.anafn.args = {scanCal.loops(2).rng, ...
    scanCal.loops(3).rng, .1, 4}; %(rngI, rngQ, radius, degree)
cal.def.configfn = [];
cal.def.configch = [];
cal.lastrun = 0;
cal.runs = [];

caldata.cals(1) = cal;

```

Data is acquired by internally calling **smrun()** with the **scan** defined in **cal.def.scan**. The acquired data is analysed by **fitRiData()**, which requires the range of I and Q

voltages, a radius for a circular mask, to exclude datapoints and degree representing the maximum order of the 2D polynomial fitted to the data. The calculated coefficients are saved into `cal.runs.params`.

4. `fitRiData()` expects real and imaginary data produced by `scanCal`. The data describing $\text{Re}_{\omega_{LO}}(I, Q)$ and $\text{Im}_{\omega_{LO}}(I, Q)$ is fitted as $\text{I}_{\omega_{LO}}(\text{Re}, \text{Im})$ and $\text{Q}_{\omega_{LO}}(\text{Re}, \text{Im})$ with a 2d polynomial using single value decomposition (svd). A mask with $\text{Rm}^2 + \text{Im}^2 < \text{radius}^2$ can be used to exclude data. `degree` is used to specify the order of the 2d polynomial.
5. `calrun()` is used to run the calibration and save the results in `caldata`:

```
calnum = 1;

calrun(calnum, '', 1); % uses smrun() to obtain data
%calrun(calnum, 'ana', 1); % uses already obtained data on disk
```

The first variant using the calibration definition defined above, starts `smrun()` to acquire data. The data is additionally saved to `caldata.iqmx/sm.iqmx_1.001.mat` the specific rules for the composition of the filename can be found in `calrun.m`.

The second variant uses an already obtained data file for analysis.

6. `plotRiData()` can be used to examine the data, the fit and residuals:

```
plotRiData(1, 'data', [3 5 7] .* 1e9);
plotRiData(1, 'fit', [3 5 7] .* 1e9);
plotRiData(1, 'resi', [3 5 7] .* 1e9);

plotRiData(1, 'gof tab', [3 5 7] .* 1e9);
```

The first argument specifies a calibration from `caldata` by index or name. The second argument specifies the type of plot. 'gof' or 'gof tab' can be used to examine the RMS and maximum values of the residuals graphically or in tabular form for different LO frequencies.

The third argument is the frequency. Using a list of frequencies for 'data', 'fit', and 'resi' will pause between every plot.

After an examination of the data, the radius of the mask or the degree of the polynomial can be adjusted and the calibration process repeated.

7. `calsave()` is used to save the calibration definition containing the calculated coefficients.
8. `smsshutdown` is used to disconnect the instruments and for general clean up.

7.2 RF pulse creation

Based on an IQ mixer calibration present in `caldata`, RF pulses or chirps can be generated using calibrated I and Q values in Pulsecontrol.

A RF pulse is a new type of pulse based on the 'elem' format defined in `plstotab.m`. It is a high-level pulse controlled by up to 9 values:

```
clear pinf;
plsnum=2;
pinf.name = 'rfPulse1';

pdstart.type = 'rfpulse';
pdstart.time = 0;
% val = [ startRfFreq, stopRfFreq, LO frequency, ...
% amplitude, phase, (calnumber, (runind))]
pdstart.val= [7e9+25e6 7e9+25e6 7e9 0.1 0 11];
pdrfpulse.type = 'rfpulse';
pdrfpulse.time = 1;
pdrfpulse.val = pdstart.val;

pinf.data = [pdstart pdrfpulse];
plsplot(pinf);
plsreg(pinf, plsnum);
```

The pulse is created out of pulseelements of the type 'rfpulse'.

`val = [...]` defines the properties. When not explicitly specifying an index in `caldata` via `calnumber`, a calibration with the name 'iqmx' from `caldata` is chosen.

To create a chirp, different `startRfFreq` and `stopRfFreq` are required. The speed of the frequency transition is controlled by the length of the pulse (`time`).

Setting `time=0` creates a start pulseelement with correct I and Q values.

The `amplitude` is set in volts (V_P). Since the AWG specifies the amplitude as a peak-to-peak value (V_{PP}), I and Q signals are internally scaled with the factor two.

`plstotab.m` implements the new type 'rfpulse' by using a helper-function called `plsIqFnCreate()`, which creates anonymous functions I and Q, using the coefficients from the calibration according to:

$$c(t) = \text{amplitude} \cdot \exp(i(2\pi(f_1 + \frac{f_2 - f_1}{\text{time}}t)t + \text{phase}))$$

$$I(t) = a_{00} + a_{01}\text{Im}(c(t)) + a_{02}\text{Im}^2(c(t)) + \dots + a_{10}\text{Re}(c(t)) + \dots$$

$$Q(t) = b_{00} + b_{01}\text{Im}(c(t)) + b_{02}\text{Im}^2(c(t)) + \dots + b_{10}\text{Re}(c(t)) + \dots$$

f_1 and f_2 are the IF frequencies obtained from the difference of RF and LO frequencies. This functions are evaluated by `plstowf.m` to actual voltages sent to the AWG.

Declaration of own work

I hereby declare that this document has been composed by myself and describes my own work, unless otherwise acknowledged in the text. It has not been accepted in any previous application for a degree. All sources of information have been specifically acknowledged in all conscience.

Aachen, 30 July 2012
Eugen Kammerloher